Masanori Akira, MD • Satoru Yamamoto, MD • Kunihiko Yokoyama, MD • Nobuhiko Kita, MD • Kenji Morinaga, MD • Tokuro Higashihara, MD • Takahiro Kozuka, MD

Asbestosis: High-Resolution CT–Pathologic Correlation[1]

High-resolution computed tomography (HRCT) was performed in seven inflated and fixed postmortem lungs from seven asbestos-exposed patients with pathologically proved asbestosis. The parenchymal abnormalities seen at in vitro HRCT included thickened intralobular lines (n = 7), thickened interlobular lines (n = 7), pleural-based opacities (n = 7), parenchymal fibrous bands (n = 5), subpleural curvilinear shadows (n = 4), ground-glass appearance (n = 4), traction bronchiectasis (n = 4), and honeycombing (n = 2). The thickened intralobular lines were shown histologically to be due to peribronchiolar fibrosis. Thickened interlobular lines were due mainly to interlobular fibrotic thickening in four lungs and edema in three. The peribronchiolar fibrosis was most severe in the subpleural lung regions, creating curvilinear line shadows and pleural-based areas of opacity. Some subpleural fibrosis extended proximally along the bronchovascular sheath to create bandlike lesions. Areas of ground-glass appearance on HRCT scans were shown to be the result of mild alveolar wall and interlobular septal thickening due to fibrosis or edema. Postmortem HRCT findings were similar to premortem HRCT findings and correlated well with the pathologic findings of asbestosis.

Index terms: Asbestosis, 60.773 • Computed tomography (CT), high-resolution • Lung, CT, 60.1211 • Lung, diseases, 60.773

Radiology 1990: 176:389–394

HIGH-RESOLUTION computed tomography (HRCT) findings in asbestosis have been well documented (1–7). Findings include thickened interlobular septal lines and intralobular core structures, parenchymal fibrous bands, honeycomb patterns, and subpleural opacities and curvilinear lines that persist in the prone position (1–3).

We previously examined paired serial HRCT scans of 23 occupational asbestos-exposed patients who showed radiographic profusion of 0 or 1, and concluded that subpleural isolated dotlike or branching structures connected with the most peripheral branch of the pulmonary artery are the earliest diagnostic HRCT findings in asbestosis.

Yoshimura et al (7) performed HRCT in 19 asbestos-exposed patients who demonstrated small, irregular opacities on standard radiographs. They noted a subpleural curvilinear shadow parallel to the inner chest wall in the lungs of 15 of the patients. Radiologic-pathologic correlation was available for one postmortem lung, and the curvilinear shadow corresponded to peribronchiolar fibrotic thickening with anthracosis, combined with flattening and collapse of the alveoli due to fibrosis. The authors suggested that the shadow might be related to early pulmonary fibrosis.

Although CT findings in asbestosis have been described, CT-pathologic correlation has not been extensively documented (8). To determine the pathologic basis for CT findings, we examined with HRCT seven inflated, fixed, and air-dried postmortem lung specimens from seven asbestos-exposed patients with pathologically proved asbestosis, and correlated the HRCT findings with the corresponding histologic findings.

MATERIALS AND METHODS

Seven lungs excised at autopsy from seven patients with asbestosis were studied. The histologic criteria described by Craighead (9) were used to diagnose asbestosis. The specimens comprised three right and four left lungs. The subjects were five men and two women whose age at death ranged from 56 to 77 years (mean, 67.6 years). Their mean duration of exposure to asbestos was 20.6 years ± 7.8 (range, 10–34 years), and the interval from first exposure to death was 30.9 years ± 6.5 (range, 20–42 years). Three subjects had never smoked. Four subjects were smokers, one of whom had stopped smoking for more than 1 year at time of death.

The lungs were fixed by the method described by Markarian and Dailey (10). Each was first distended through a main bronchus with fixative fluid containing polyethylene glycol 400, 95% ethyl alcohol, 40% formalin, and plain water in proportions of 10:5:2:3, and immersed in the fixative for 2 days. The fixed lung was then air dried and cut into sagittal (n = 5) or transaxial slices (n = 2) 0.5 cm thick. A radiograph of each slice was obtained with a fine-grain film (Softex; Fuji, Tokyo) at 20 kVp and 250 mAs, with a source-film distance of 60 cm. The specimens were then scanned with a GE 8800 scanner (GE Medical Systems, Milwaukee), with 1.5-mm-thick sections and targeted reconstruction (by means of a convolution filter) of the bone-detail algorithm, with a field of view of 16–25 cm, depending on the size of the lung. In vitro HRCT scans were graded by two observers (M.A., T.H.), and their consensual grade was recorded. The severity of each kind of abnormality was scored on a 4-point scale for each lung slice: − (normal), + (slight, <25%), ++ (moderate, 25%–50%), and +++ (prominent, >50%).

Abbreviation: HRCT = high-resolution computed tomography.

[1] From the Departments of Radiology (M.A.), Pathology (S.Y.), and Medicine (K.Y., N.K., K.M.), National Kinki Chuo Hospital for Chest Diseases, 1180 Nagasone-cho, Sakai City, Osaka 591, Japan; the Department of Radiology, Kansai Rosai Hospital, Amagasaki, Japan (T.H.); and the Department of Radiology, Osaka University Medical School, Osaka, Japan (T.K.). Received December 20, 1989; revision requested January 30, 1990; revision received March 26; accepted April 19. **Address reprint requests to** M.A.

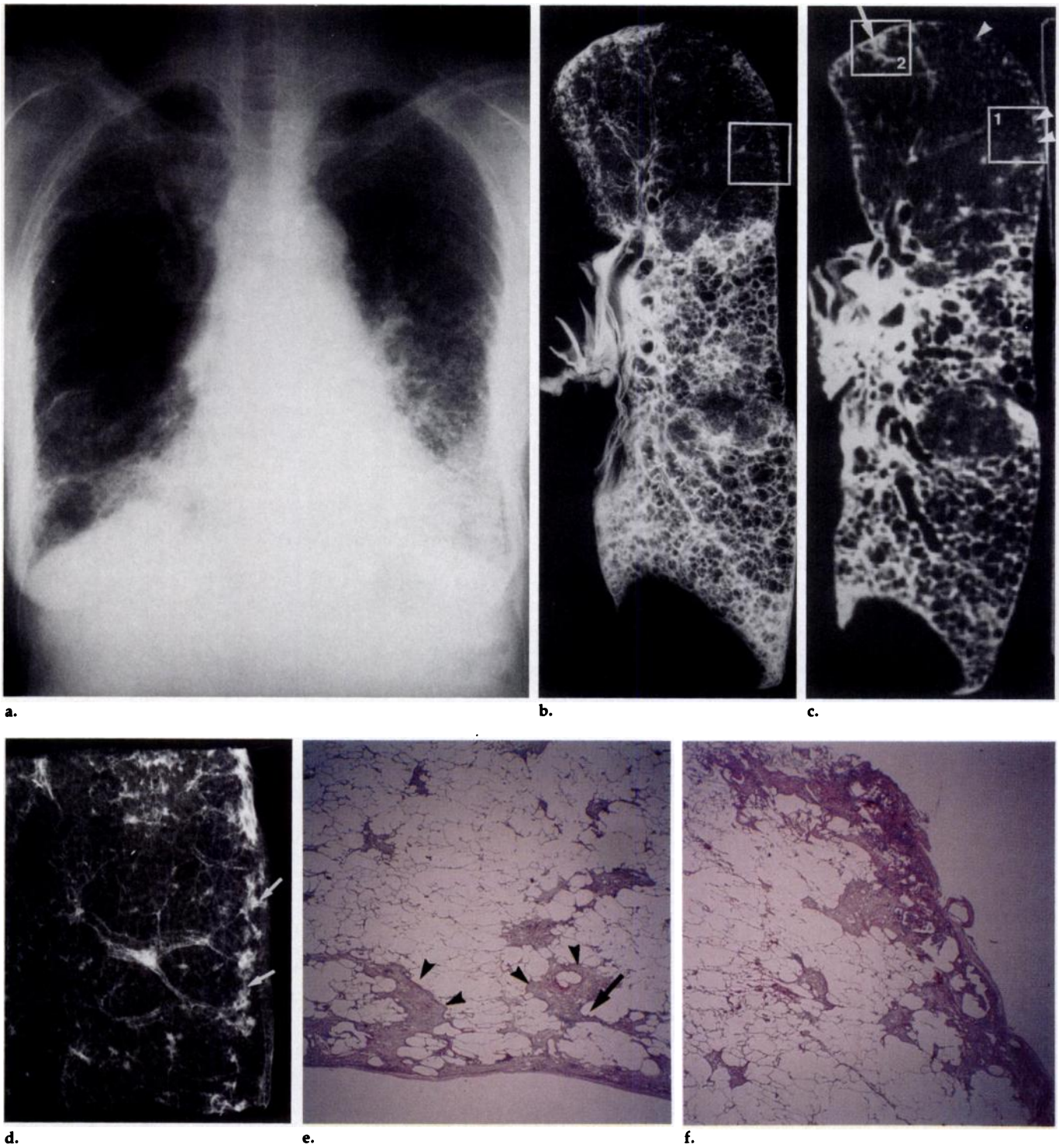

Figure 1. Images from woman who died at the age of 75 years after 31 years in the asbestos textile industry and 25 years of exposure. She had never smoked. **(a)** Chest radiograph obtained 1 month before death shows diffuse, small, irregular opacities (coarse reticular pattern; profusion, 2/3). This patient also had primary squamous cell carcinoma in the right lower lobe. Postmortem low-kilovoltage radiograph **(b)** and HRCT scan **(c)** of the inflated and fixed left lung show honeycombing in the lower two-thirds of the lung. In the subpleural zones, dotlike lesions (arrowheads), confluence of dots, and a pleural-based, wedge-shaped opacity (arrow) are seen. **(d)** Magnified view of box in **b.** Nodular opacities can be seen a few millimeters from the pleural surface and are joined with adjacent nodular opacities and the visceral pleural surface by linear opacities (arrows). **(e)** Photomicrograph of lung specimen obtained from box *1* in **c.** Peribronchiolar nodular fibrosis (arrowheads) is seen along the pleural surface. Part of lesion is attached to the visceral pleura. Arrow indicates the bronchiole (hematoxylin-eosin stain; original magnification, ×2.5). **(f)** Photomicrograph of lung specimen obtained from box *2* in **c.** Subpleural fibrosis and peribronchiolar fibrosis are joined (hematoxylin-eosin stain; original magnification, ×2.5).

The final score for each parenchymal abnormality was calculated by assessment of the percentage of involvement in each lung slice and multiplication by a factor to correct for differences in volumes among the slices. Areas of low attenuation suggestive of emphysema and bullae were not evaluated. Tissue blocks for histologic examination were selected on the basis of the CT images. In vitro HRCT findings were correlated with findings in the corresponding histologic sections.

Table 1
Frequency and Degree of Parenchymal Abnormalities on Postmortem HRCT Scans of Lungs with Asbestosis

Case	Thickened Intralobular Lines	Thickened Interlobular Lines	Pleural-based Opacities	Parenchymal Bands	Subpleural Curvilinear Shadows	Traction Bronchiectasis	Ground-Glass Appearance	Honeycombing
1	++	++	+	+++	+	++	−	+
2	+++	+++	++	+	+	−	++	−
3	+++	++	++	+	+	−	++	−
4	++	++	+	−	−	+	+	−
5	++	+	++	−	−	−	−	+++
6	+++	+	+++	++	+	+	+	−
7	++	+	+	+	−	+	−	−
Total	7	7	7	5	4	4	4	2

Note.—− = not found; + = slight, <25%; ++ = moderate, 25%–50%; +++ = prominent, >50%.

Table 2
HRCT-Pathologic Correlation

HRCT Sign	Pathologic Correlate
Thickened intralobular lines	Peribronchiolar fibrosis with subsequent involvement of the alveolar ducts
Thickened interlobular lines	Interlobular fibrotic thickening or edematous thickening
Pleural-based opacities	Subpleural fibrosis
Parenchymal bands	Fibrosis along the bronchovascular sheath or interlobular septa, with distortion of the parenchyma
Ground-glass appearance	Mild alveolar wall and interlobular thickening by fibrosis or edema
Subpleural curvilinear lines	Peribronchiolar fibrotic thickening combined with flattening and collapse of the alveoli due to fibrosis

RESULTS

The parenchymal abnormalities seen at in vitro HRCT and their frequency and degree are listed in Table 1. The parenchymal abnormalities included thickened intralobular lines (n = 7), thickened interlobular lines (n = 7), pleural-based opacities (n = 7), parenchymal fibrous bands (n = 5), subpleural curvilinear shadows (n = 4), ground-glass appearance (n = 4), traction bronchiectasis (n = 4), and honeycombing (n = 2). Predominant sites of lesions were the posterior lower zones.

Thickened intralobular lines, thickened interlobular lines, and pleural-based opacities were seen in all lungs. All the thickened intralobular lines showed predominant subpleural distribution, and in three lungs also severely affected the central portions. The subpleural lesions appeared as dotlike structures a few millimeters from the pleural surface in less abnormal areas (Fig 1d). The subpleural dotlike structures were arranged along the inner chest wall and resembled a curvilinear shadow. Clusters of subpleural dots were confluent, and the confluence created the pleural-based opacities (Fig 1b, 1c). Histologically, the dotlike lesions corresponded to peribronchiolar nodular fibrosis with subsequent involvement of the alveolar ducts (Fig 1e). In all subjects, although peribronchiolar fibrosis was seen from site to site histologically, the disease was so severe in the subpleural portion that it could be recognized as a dotlike structure at HRCT (Fig 1c).

The pleural-based opacities corresponded to subpleural pulmonary fibrosis histologically (Figs 1f, 2d). Some areas of opacity were wedge-shaped or lamellar structures that lined the pleural surface (Fig 1b), and some extended proximally along the bronchovascular sheath to show bandlike lesions (Fig 3c). Parenchymal fibrous bands extended almost along the bronchovascular sheath, but some were associated with distortion of the parenchyma caused by traction of the thickened pleura and fibrous thickening of interlobular septa.

The thickened interlobular lines were seen in all seven lungs. In four lungs, they corresponded histologically to mainly interlobular fibrotic thickening, and in the rest to interlobular edematous thickening. The ground-glass appearance was seen in four of seven lungs. This appearance corresponded histologically to the thickening of alveolar walls by fibrosis or edema (Fig 2e). Interlobular septa that were thickened by fibrosis or edema but were not prominent enough to be recognized as short lines at HRCT created the ground-glass appearance. Mild thickening of the alveolar walls, especially when lung architecture was preserved, was seen as normal lung at HRCT.

The pathologic bases of the HRCT findings are presented in Table 2.

DISCUSSION

Several studies have addressed the application of HRCT to the evaluation of pulmonary asbestosis. Findings at HRCT included curvilinear subpleural lines (7), thickened interlobular septal lines, thickened intralobular lines, parenchymal fibrous bands, subpleural dependent opacities, honeycomb pattern (1–3), and pleural-based nodular irregularities. Yoshimura et al (7) showed that the subpleural curvilinear shadow corresponded to peribronchiolar fibrotic thickening with anthracosis, combined with flattening and collapse of the alveoli due to fibrosis. However, the literature lacks good studies with pathologic correlation of the radiologic signs of asbestosis seen on HRCT scans.

The fibrotic process of asbestosis begins in the peribronchiolar areas of the lung, then progresses to involve adjacent alveoli, showing the classic features of asbestosis (interstitial fibrosis) (9). Asbestosis is usually more severe in the lower subpleural zones (9). Animal experiments have indicated that the initial sites of asbestos fiber deposition are the respiratory bronchioles and alveolar ducts (11) and that, with time, asbestos fibers tend to concentrate under the pleura (12). Our preliminary data showed that the early parenchymal changes seen on HRCT scans are subpleural isolated dotlike structures connected to the most peripheral branch of the pulmonary artery, and that these dots increase in number to create a reticulonodular appearance on serial HRCT scans. In all seven inflated and

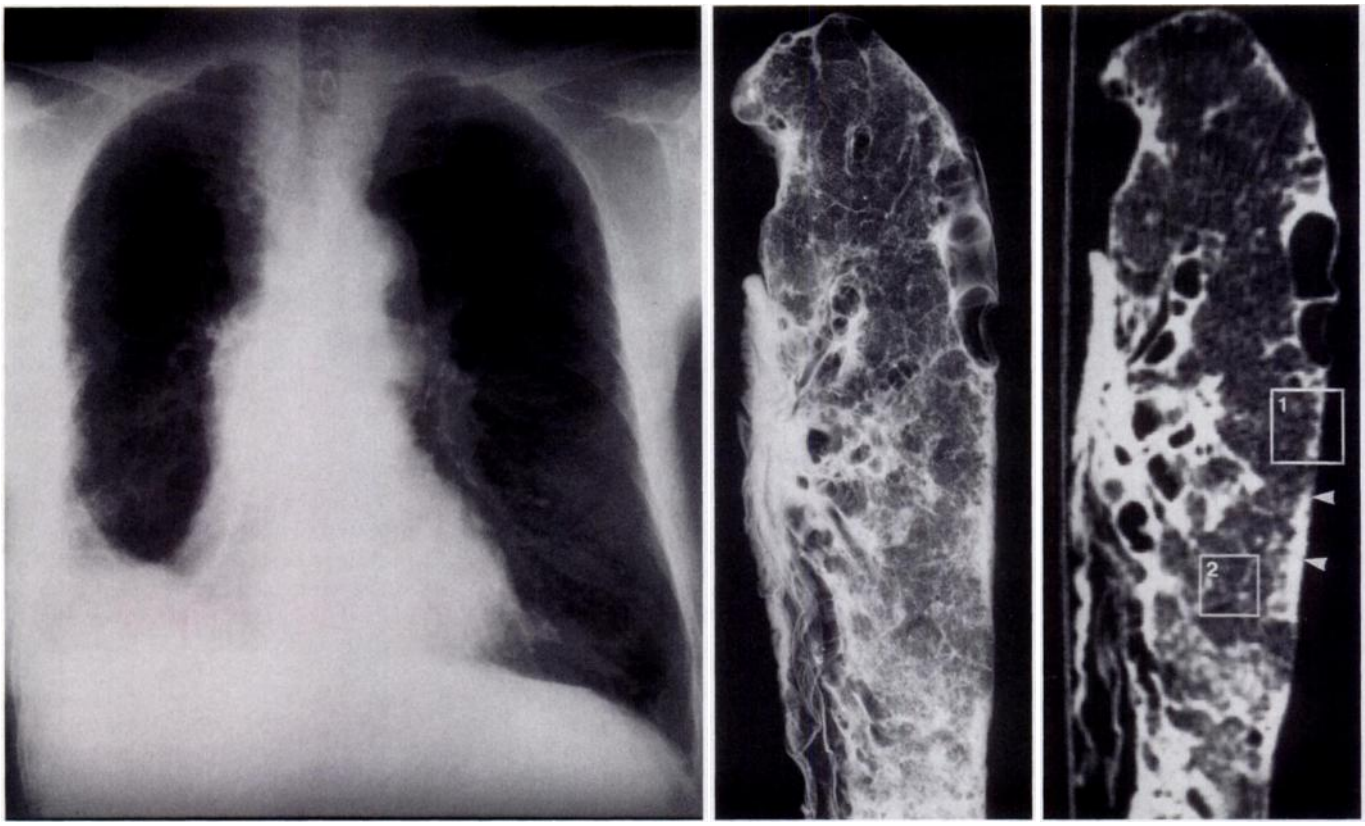

a. b. c.

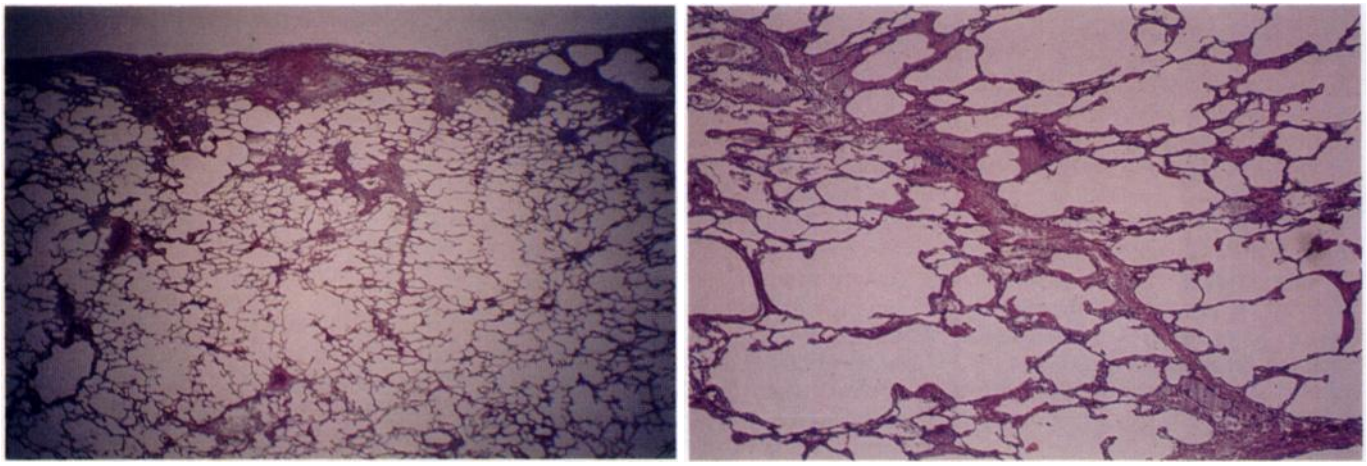

d. e.

Figure 2. Images from man who died of carcinoma of the stomach at the age of 68 years after 10 years in the asbestos textile industry. He had undergone a right lower lobectomy due to bronchogenic carcinoma in the right lower lobe 8 years before. **(a)** Chest radiograph obtained 1 month before death shows small round opacities (fine nodular pattern; profusion, 1/1) as well as small, irregular opacities. Postmortem low-kilovoltage radiograph **(b)** and HRCT scan **(c)** of the inflated and fixed left lung show intralobular and interlobular thickenings, subpleural opacities (arrowheads), and areas with a ground-glass appearance (box *2*). **(d)** Photomicrograph of lung specimen obtained from box *1* in **c.** Subpleural fibrosis and peribronchiolar fibrosis are seen (hematoxylin-eosin stain; original magnification, ×2.5). **(e)** Photomicrograph of lung specimen obtained from box *2* in **c.** The thickenings of interlobular septa and alveolar walls by edema are seen (hematoxylin-eosin stain; original magnification, ×10).

fixed postmortem lungs, we observed similar subpleural dotlike structures in less abnormal areas of in vitro HRCT scans, and these dots corresponded to peribronchiolar nodular fibrosis with subsequent involvement of the alveolar ducts histologically. In all lungs, although peribronchiolar fibrosis was seen from site to site histologically, the peribronchiolar fibrosis in the subpleural portion was of a degree that could be recognized as a dotlike structure at HRCT. Peribronchiolar fibrosis obliterated surrounding alveoli, extending outward from the bronchiole and joining adjacent peribronchiolar fibrosis and the visceral pleura. It was thought that the subpleural dots arranged along the inner chest wall created a subpleural curvilinear shadow. The confluence of these subpleural dots was thought to result in a lamellar structure of subpleural pulmonary fibrosis.

We previously observed the pleural-based wedge-shaped opacity on HRCT scans of asbestos-exposed patients with early parenchymal abnormalities (6). The same opacities seen

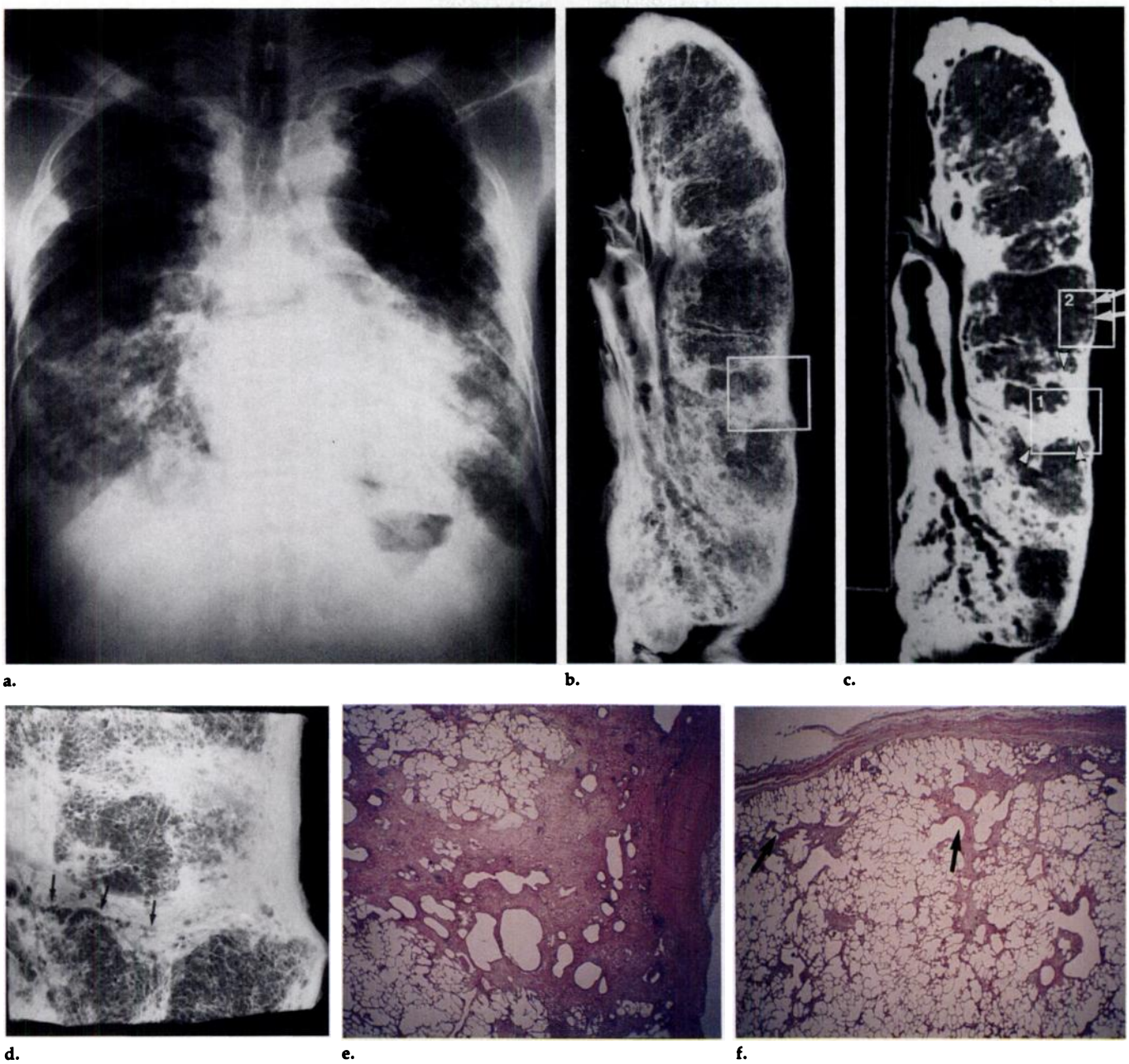

Figure 3. Images from man who died at the age of 56 years after 42 years in the asbestos textile industry and 22 years of exposure. **(a)** Chest radiograph obtained 1 month before death shows a predominantly basal involvement, "shaggy" heart, and extensive bilateral pleural thickening (profusion, 3+). The right interlobar fissure is thickened. Postmortem low-kilovoltage radiograph **(b)** and HRCT scan **(c)** of the inflated and fixed left lung show diffuse pleural thickening and pleural-based opacities extending along the bronchovascular sheath (arrowheads). Subpleural nodular opacities are also seen (arrows). **(d)** Magnified view of box in **b**. The bronchus is seen in the area of increased opacity (arrows). **(e)** Photomicrograph of lung specimen obtained from box *1* in **c**. Pleural fibrosis and fibrosis along the bronchovascular sheath are seen (hematoxylin-eosin stain; original magnification, ×2.5). **(f)** Photomicrograph of lung specimen obtained from box *2* in **c**. Subpleural fibrosis and peribronchiolar nodular fibrosis are joined. Arrows indicate the bronchioles (hematoxylin-eosin stain; original magnification, ×2.5).

on in vitro HRCT scans corresponded to subpleural pulmonary fibrosis histologically. These opacities were seen in all the lungs, despite differences in degree. Some extended proximally along the bronchovascular sheath to show bandlike lesions. Parenchymal fibrous bands coursed almost along the bronchovascular sheath or interlobular septa, even though their directions appeared to be incompatible with those of blood vessels. Some areas of opacity due to subpleural pulmonary fibrosis were the lamellar structures lining the pleura surface, which attached to pleural fibrosis to create the thickenings of the axillary pleural line and interlobar area that could be recognized on radiographs. Thickening of the axillary pleural line was due to pleural thickening or subpleural pulmonary fibrosis or both. Subpleural pulmonary fibrosis could not easily be differentiated from pleural thickening. Prominent irregularity of the pleural surface suggested that the thickening was due to subpleural fibrosis.

Alveolar walls thickened by fibrosis or edema and interlobular septal thickenings that were not prominent enough to be recognized as short lines at HRCT, in addition to aeration of alveolar spaces, may have created the ground-glass appearance. Mild thickening of the alveolar walls, especially when lung architecture was preserved, was seen as normal-appearing lung at HRCT.

In the lungs we examined, predeath agonal events may have occurred and modified the pathologic findings. Evidence of interstitial edema seen in case 3 (Table 1) was considered as due to a complicating agonal event.

In conclusion, our study of the HRCT-pathologic correlation in asbestosis showed that HRCT findings correlated well with the pathologic findings of asbestosis and that HRCT is useful in the evaluation of parenchymal changes in asbestosis. ■

References

1. Gamsu, G, Aberle DR, Lynch D. Computed tomography in the diagnosis of asbestos-related thoracic disease. J Thorac Imaging 1989; 4:61–67.
2. Aberle DR, Gamsu G, Ray CS, Feuerstein IM. Asbestos-related pleural and parenchymal fibrosis: detection with high-resolution CT. Radiology 1988; 166:729–734.
3. Aberle DR, Gamsu G, Ray CS. High-resolution CT of benign asbestos-related diseases: clinical and radiographic correlation. AJR 1988; 151:883–891.
4. Friedman AC, Fiel SB, Fisher MS, et al. Asbestos-related pleural disease and asbestosis: a comparison of CT and chest radiography. AJR 1988; 150:269–275.
5. Lynch DA, Gamsu G, Ray CS, Aberle DR. Asbestos-related focal lung masses: manifestations on conventional and high-resolution CT scans. Radiology 1988; 169:603–607.
6 Akira M, Yokoyama K, Higashihara T, et al. Early asbestosis: evaluation with high-resolution CT. Radiology (in press).
7. Yoshimura H, Hatakeyama M, Otsuji H, et al. Pulmonary asbestosis: CT study of curvilinear shadow. Radiology 1986; 158:653–658.
8. McLoud T. The use of CT in the examination of asbestos-exposed persons. Radiology 1988; 169:862–863.
9. Craighead JE. The pathology of asbestos-associated disease of the lungs and pleural cavities—diagnostic criteria and proposed grading schema: report of the Pneumoconiosis Committee of the College of American Pathologists and National Institute for Occupational Safety and Health. Arch Pathol Lab Med 1982; 106:544–596.
10. Markarian B, Dailey ET. Preparation of inflated lung specimens. In: Heitzman ER, ed. The lung: radiologic-pathologic correlations. 2nd ed. St Louis: Mosby, 1984; 4–12.
11. Brody AR, Hill LH, Adkins B, et al. Chrysotile asbestos inhalation in rats: deposition pattern and reaction of alveolar epithelium and pulmonary macrophages. Am Rev Respir Dis 1981; 123:670–679.
12. Morgan A, Evans JC, Holmes A. Deposition and clearance of inhaled fibrous minerals in the rat: studies using radioactive tracer techniques. In: Walton WH, McGovern B, eds. Inhaled particles IV, part 2. New York: Pergamon, 1977; 259–274.